# ELECTRONIC SUPPLEMENTARY INFORMATION

# Chiral Organocatalysts Based on Lipopeptide Micelles for Aldol Reactions in Water

Bruna M. Soares,[a] Andrea M. Aguilar,[b] Emerson R. da Silva,[c] Mauricio D. Coutinho-Neto,[a] Ian W. Hamley,[d] Mehedi Reza,[e] Janne Ruokolainen,[e] Wendel A. Alves[a]*

[a] Centro de Ciências Naturais e Humanas, Universidade Federal do ABC, Santo André 09210-580, Brazil.
[b] Instituto de Ciências Ambientais, Químicas e Farmacêuticas, Universidade Federal de São Paulo, Diadema 09972270, Brazil.
[c] Departamento de Biofísica, Universidade Federal de São Paulo, São Paulo 04023-062, Brazil.
[d] Department of Chemistry, University of Reading, Whiteknights, Reading RG6 6AD, United Kingdom.
[e] Department of Applied Physics, Aalto University School of Science, P. O. Box 15100, FI-00076, Finland.

*wendel.alves@ufabc.edu.br

## HIGH RESOLUTION MASS SPECTROMETRY OF THE LIPOPEPTIDE

PRW-$C_{16}$ - $[M + H]^+$

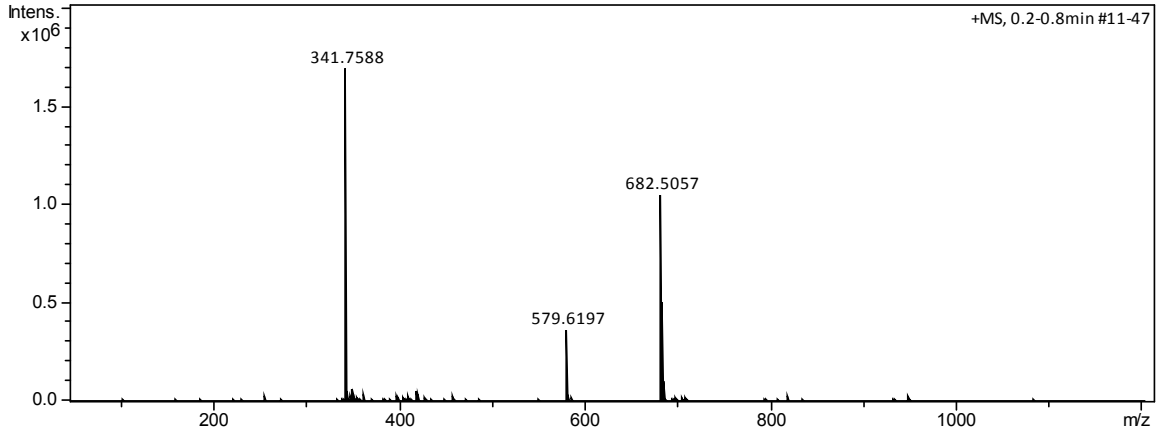


**Figure S1.** High resolution mass spectrometry of PRW-$C_{16}$. Exact mass: calculated: 681.4942; observed $[M + H]^+$: 682.5057

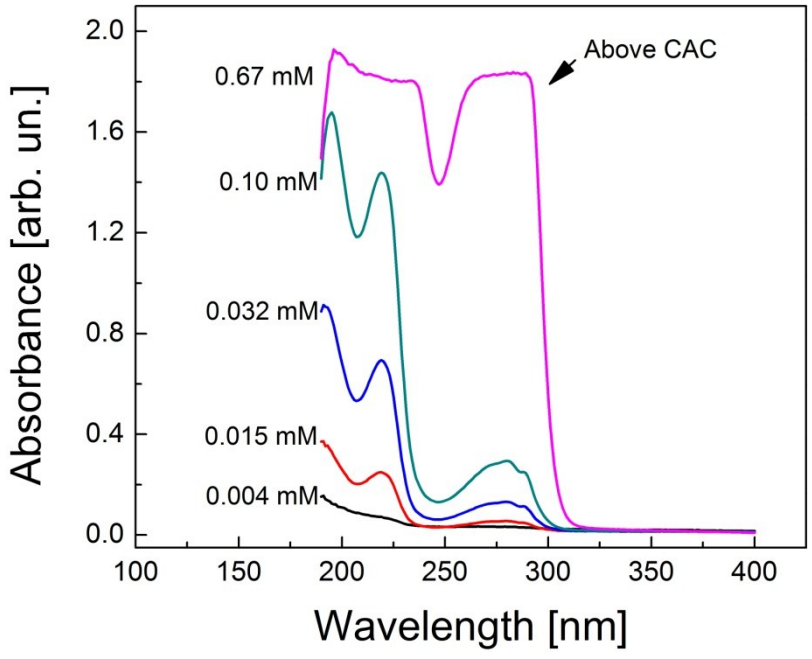


**Figure S2.** Estimation on critical concentrations of PRW-$C_{16}$ by UV-Vis spectrophotometry at different concentrations.

**SAXS MODELING**

The total scattering intensity from a sample containing a collection of identical particles is given by:

$$I(q) = N(\Delta\rho)^2 V^2 [P(q) \times S(q)] \qquad (1)$$

where *N* accounts for the concentration of particles in the medium, *V* is related to their volume and $\Delta\rho$ is the electron contrast between particles and solvent. *P(q)* is the form factor associated to electron density profile of scatterers and *S(q)* is the structure factor describing inter-particle correlation. In the dilute regime, *S(q)* → 1 and scattering intensities can described only by the form factor of the particles.

***Spherical shell form factor:***

The form factor of a homogeneous sphere is given by:[1, 2]

$$P_{sph}(q,R) = \left|\frac{3[\sin(qR) - qR\cos(qr)]}{(qR)^3}\right|^2 \qquad (2)$$

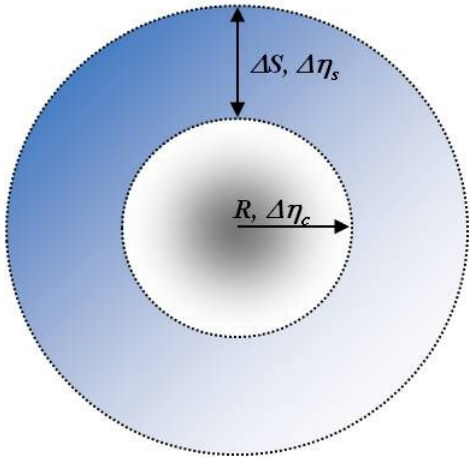


**Figure S3**. Scheme of the spherical shell used for deriving the core-shell model used in the fitting of SAXS data, with the respective parameters.

The form factor of a spherical shell, schematically represented in Fig. S2, is straightforwardly obtained by subtracting a spherical core with different electron density contrast:

$$P_{shell}(q,R,\Delta S,\Delta\eta_c,\Delta\eta_S) =$$

$$16\pi^2\left|(R+\Delta S)^3\Delta\eta_S\frac{sinq(R+\Delta S)\text{ - }qRcos(qR)}{[q(R+\Delta S)]^3}\text{ - }R^3\Delta\eta_C\frac{\sin(qR)\text{ - }qRcos(qR)}{(qR)^3}\right|^2 \quad (3)$$

***Mass fractal form factor:***

In the case of irregular aggregates, the form factor has been described by a mass fractal geometry.[3, 4] In this case, scattered intensities are generally given by:[5, 6]

$$I(q) = 4\pi\int_0^\infty g(r)r^2\frac{sin(qr)}{qr}dr \quad (4)$$

where:

$$g(r) \sim r^{D\text{ - }d}\,\mathrm{h}(r,\xi) \quad (5)$$

*D* is the fractal dimension of aggregates and *d* is the spatial dimension.[6] $\mathrm{h}(r,\xi)$ is the so-called cut-off function and it accounts for the electron density describing the perimeter of the aggregate. In the case of the form factor used in this work, the cut-off function has been chosen to be Gaussian:[3, 6]

$$\mathrm{h}(r,\xi) \sim exp\left[\text{ - }\left(\frac{r}{\xi}\right)^2\right] \quad (6)$$

With:

$$\xi^2 = \frac{4R_g^2}{D} \qquad (7)$$

Substitution of equations (5)-(7) into equation (4) leads to:[6]

$$I_{frac}(q) = exp\left[-\frac{q^2R_g^2}{D}\right]F_1^1\left[\frac{3-D}{2}, \frac{3}{2}, \frac{q^2R_g^2}{D}\right] \qquad (8)$$

Where $F_1^1$ is the confluent hypergeometric function of the first kind.[7, 8]

***Hard spheres structure factor:***

In concentrated samples, interactions between scattering centers appear in the medium and a structure factor needs to be introduced for describing inter-particle correlations. Here, we have chosen a hard sphere structure factor considering a potential of impenetrable spheres with radius $R_{HS}$:

$$U(r) = \begin{matrix} \infty \; for \; 0 < r < R_{HS} \\ 0 \; for \; r > R_{HS} \end{matrix} \qquad (9)$$

The model, calculated in the Percus-Yenick approximation,[1, 9, 10] is given by:

$$S_{HS}(q, R_{HS}, f_p) = \frac{1}{1 + 24f_p\frac{G(f_p, R_{HS}\, q)}{R_{HS}q}} \qquad (10)$$

In equation (10), $f_p$ is the volume fraction of particles and $G$ is given by:

$$G(A) = \alpha\frac{\sin(A) - A\cos(A)}{A^2} + \beta\frac{2A\sin(A) + (2 - A^2)\cos(A) - 2}{A^3} + \gamma\frac{-A$$

(11)

The coefficients $\alpha$,$\beta$ and $\gamma$ are given by:

$$\alpha = \frac{(1 + 2f_p)^2}{(1 - f_p)^4} \quad (12)$$

$$\beta = -6f_p\frac{(1 + {f_p}/{2})^2}{(1 - f_p)^2} \quad (13)$$

$$\gamma = \frac{\alpha f_p}{2} \quad (14)$$

## SMALL-ANGLE NEUTRON SCATTERING (SANS) DATA

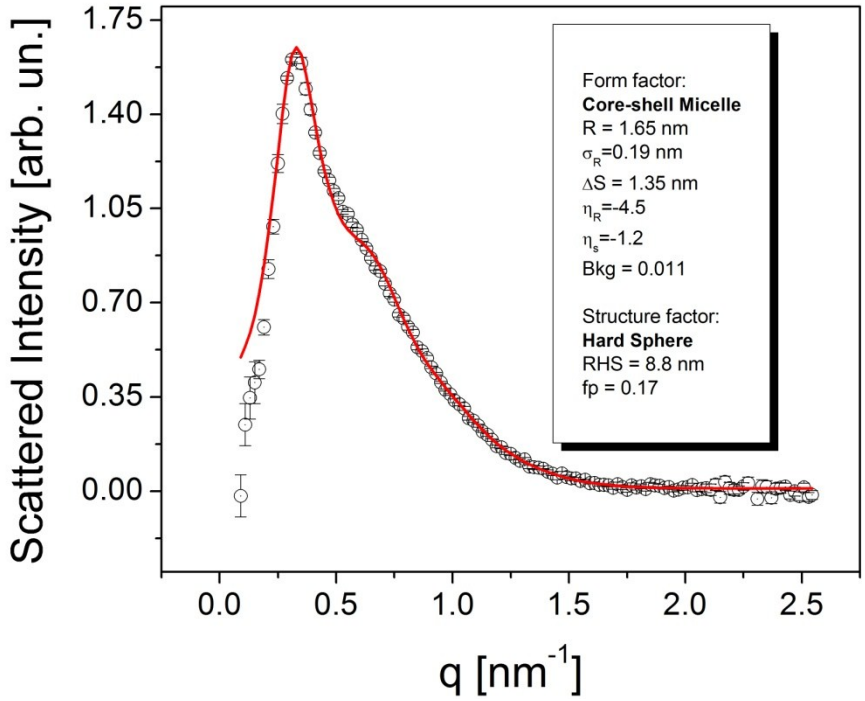


**Figure S4.** SANS profile from a 15 mM PRW-$C_{16}$ solution prepared into $D_2O$. Parameters arising from model fitting are displayed in the figure and they exhibit correspondence with values shown in Table 1 of the main text. Fit has been made with the core-shell form factor described in Eq. (3), convoluted with the hard spheres structure factor shown in Eq. (10).

**DLS ASSAYS**

Dynamic light scattering assays were performed using a solution containing lipopeptides at a concentration of 15 mM. To overcome inter-particle interactions, and thus keep validity of the dilute model used for determining hydrodynamic radii, we introduced NaCl at a concentration of 80 mM to screen electrostatic charges responsible for inter-micelle repulsion.

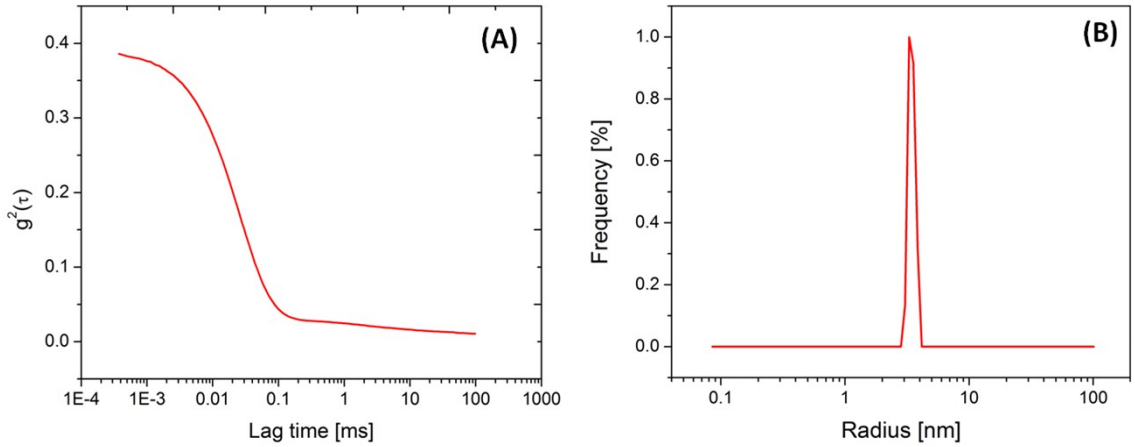


**Figure S5.** Dynamic light scattering data from a 15 mM lipopeptide solution. Hydrodynamic radii were found averaging around 3.4 nm and polydispersity of ~12 %.

## MOLECULAR DYNAMICS SIMULATIONS

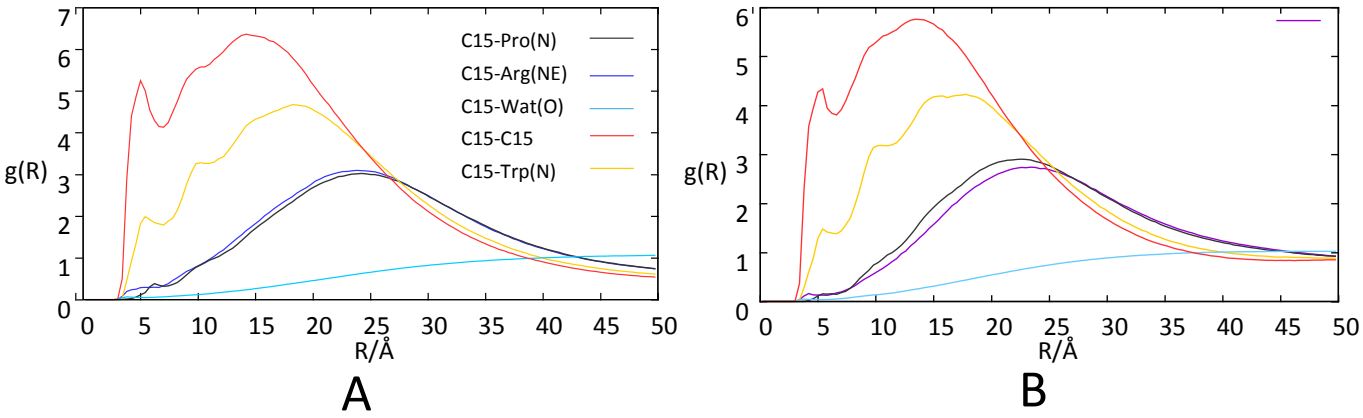


**Figure S6.** Radial distribution functions (g(R)) for water (panel A) and water cyclohexanone mixtures (panel B). All g(r) were computed with respect to carbon 15 (C15) from PRW-$C_{16}$. C15-Pro(N) (gray) refers to the distribution related to the C15/Proline nitrogen pair, C15-Arg(NE) to C15/Arginine sidechain nitrogen pair, C15-Trp(N) (yellow) to C15/Tryptophan sidechains nitrogen pair, C15-Wat(O) (blue) to C15/Water oxygen pair and C1-C15 (red) to C1/C15 pair from PRW-$C_{16}$ alkyl's chain. No intra-molecular pairs were considered when computing the RDFs.

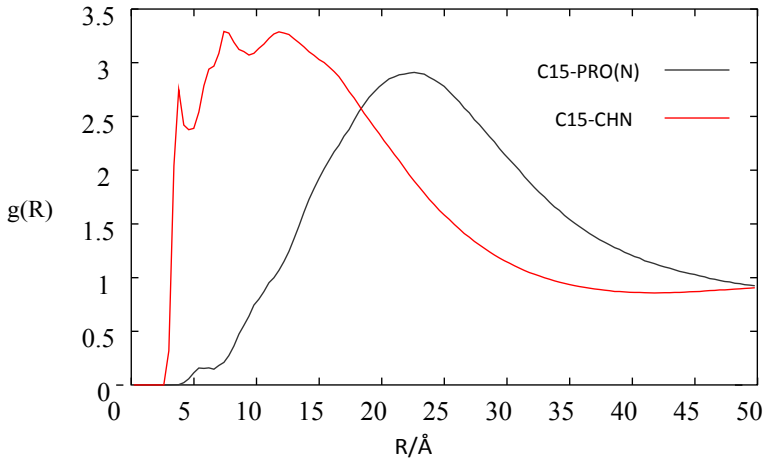


**Figure S7.** Radial distribution functions (g(R)) for a simulation using a water cyclohexanone mixture (simulation B). All g(r) were computed with respect to carbon 15 (C15) from PRW-$C_{16}$. C15-CHN (red) refers to the distribution related to the C15/cyclohexanone oxygen pair while C15-PRO(N) (gray) refers to the distribution related to the C15/Proline nitrogen pair.

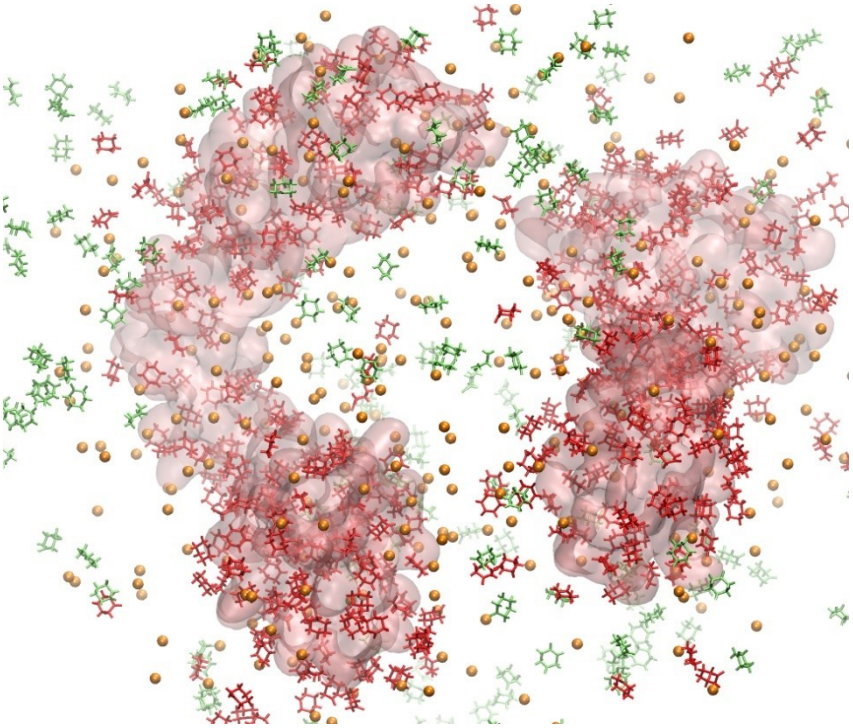

**Figure S8.** Cyclohexanone distribution in the simulation box from simulation B after 50 ns. The cyclohexanones were drawn using a bond representation in red and in green depending on their distance from the alkyl chains. The alkyl chains were drawn using a surface representation in pink.

## SPECTROSCOPIC AND CHIRAL-HPLC ANALYSIS FOR THE ALDOL PRODUCT

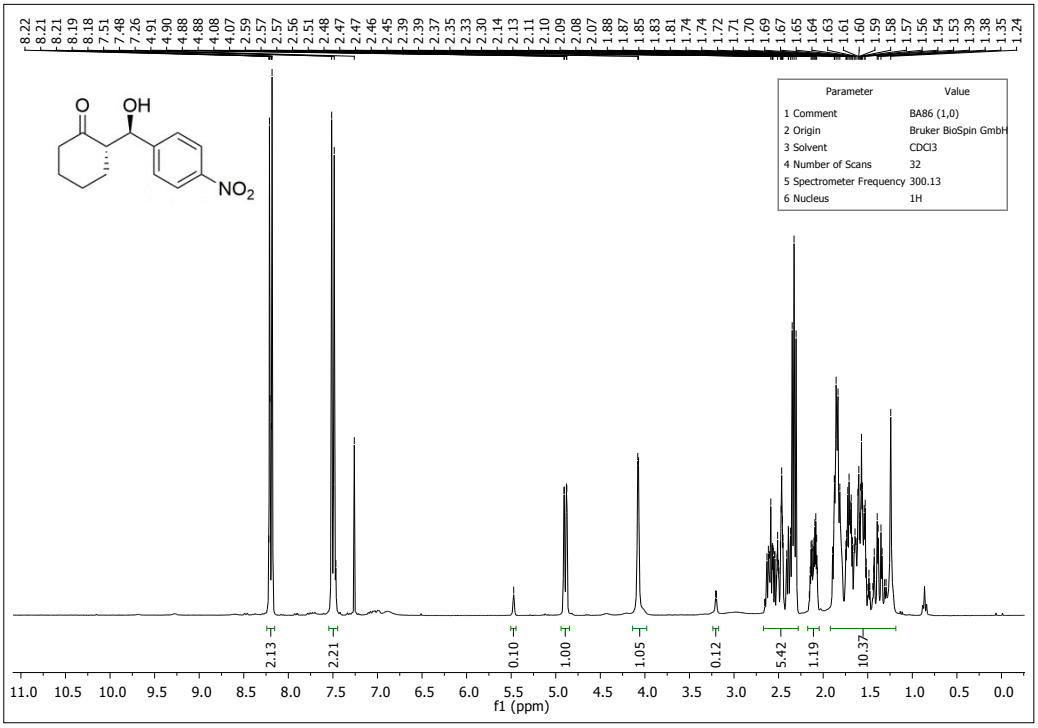


**Figure S9.** $^{1}$H NMR spectrum of the crude aldol product ($CDCl_3$, 300 MHz).

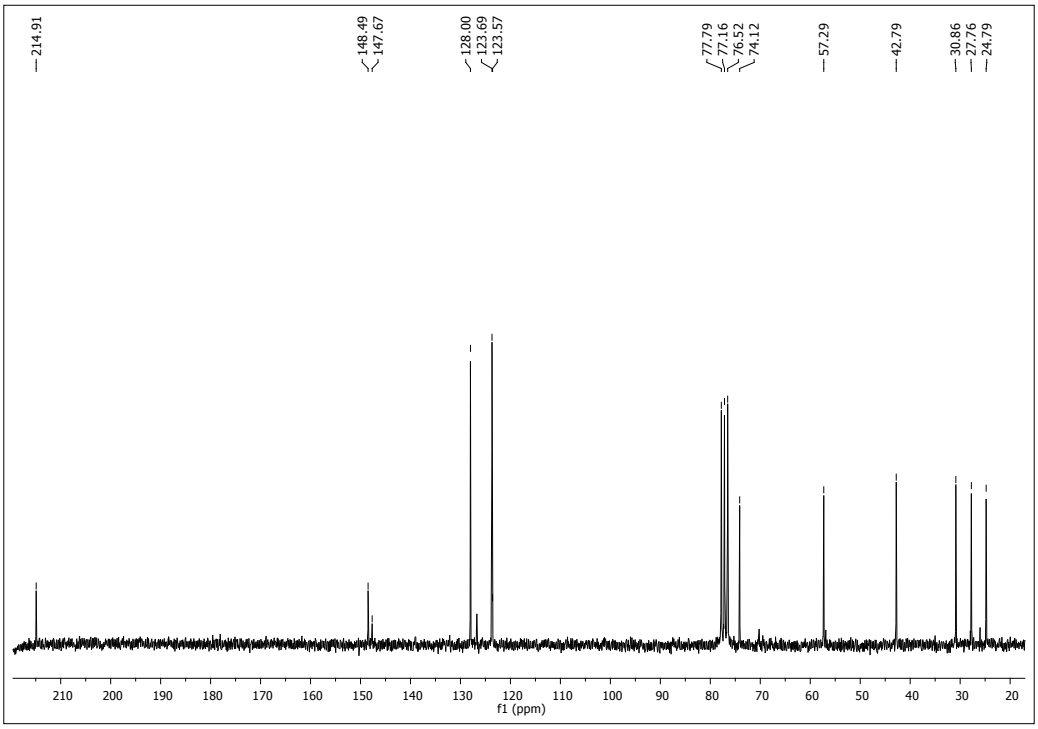


**Figure S10.** $^{13}$C NMR spectrum of the aldol product ($CDCl_3$, 50 MHz).

***Spectroscopic Data***

**(*S*)-2-((*R*)-Hydroxy(4-nitrophenyl)methyl)cyclohexan-1-one**

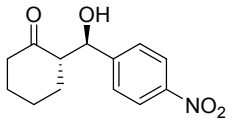


**$^{1}$H NMR** (300 MHz, $CDCl_3$): δ 8.22-8.18 (m, 2H, ArH); 7.51-7.47 (m, 2H, ArH); 5.47 (br s, 1H, C*H*OH-*syn*); 4.89 (dd, *J* = 7.5 Hz, 3.0 Hz, 1H, C*H*OH-*anti*); 4.08 (d, *J* = 3.0 Hz, 1H, CHO*H*-*anti*); 3.21 (d, *J* = 3.0 Hz, 1H, CHO*H*-*syn*); 2.66-2.30 (m, 1H, C*H*CHOH); 2.66-2.30 (m, 2H, $CH_2C(O)$); 2.16-1.24 (m, 6H, chex-H).

**$^{13}$C NMR** (50 MHz, $CDCl_3$): δ 214.9 (C=O); 148.5 (ArC); 147.7 (ArC); 128.0 (2 x ArCH); 123.7 (2 x ArCH); 74.1 (CHOH); 57.3 (*C*HCHOH); 42.8 ($CH_2$); 30.9 ($CH_2$); 27.8 ($CH_2$); 24.8 ($CH_2$).

**Table S1.** $^{1}$H NMR C*H*OH (δ ppm) and HPLC conditions and retention times for the aldol product.[11]

| **$^{1}$H NMR ($CDCl_3$, -C*H*OH, δ ppm, *J* Hz)** | | **HPLC** | | | |
|---|---|---|---|---|---|
| ***syn*** | ***anti*** | **Column** | **Eluent and Flow rate** | ***syn*** **t (min)** | ***anti*** **t (min)** |
| 5.47 (br s) | 4.89 (dd, *J* = 7.5 Hz, 3.0 Hz) | CHIRALPAK AD-H | Hexane/2-propanol (90/10); 1.0 mL/min | 17.297 (minor) 21.520 (major) | 23.331 (2*S*, 1'*R*) 30.937 (2*R*, 1'*S*) |

***Diastereomeric ratio determined by $^{1}H$ NMR spectroscopic analysis***

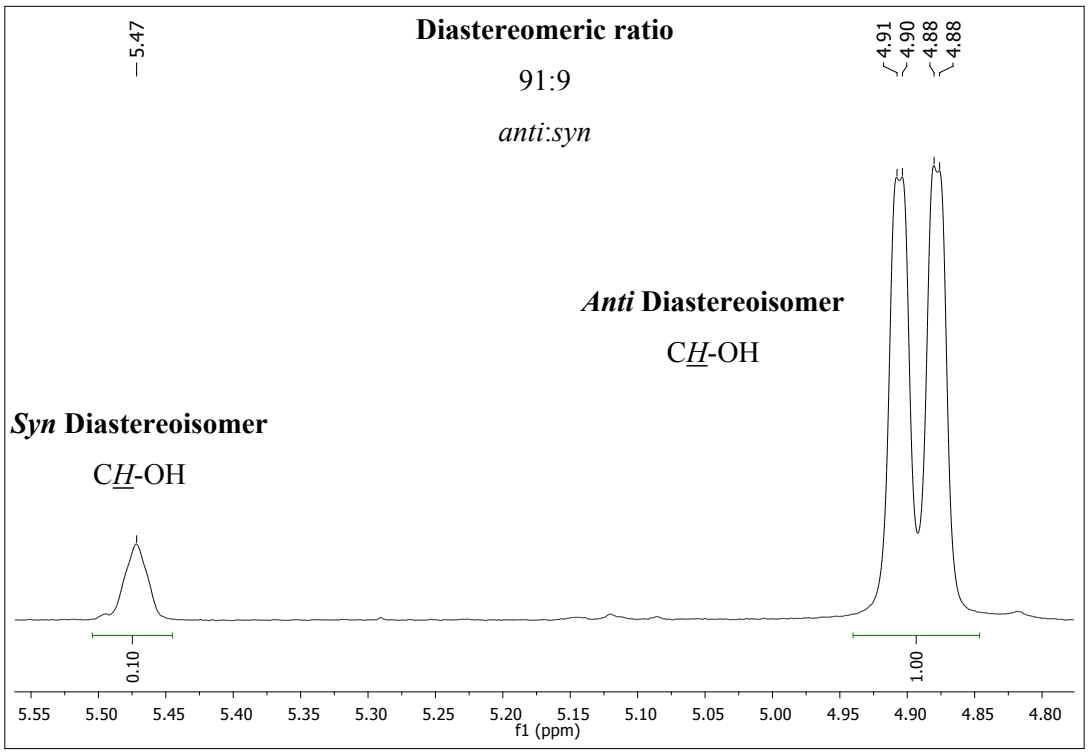

***Enantiomeric excess determined by chiral-phase HPLC analysis***

**==== Shimadzu LCsolution Analysis Report ====**

C:\LabSolutions\Data\Profa Andrea\Elaine\Aldol_rac.lcd

| | |
|---|---|
| Acquired by | : Admin |
| Sample Name | : Aldol_rac |
| Sample ID | : Aldol_rac |
| Tray# | : 1 |
| Vail # | : 1 |
| Injection Volume | : 1 uL |
| Data File Name | : Aldol_rac.lcd |
| Method File Name | : Chiral_AD-H_10-90_1.0mL-min-40min-08out2014.lcm |
| Batch File Name | : batch-08out2014.lcb |
| Report File Name | : Default.lcr |
| Data Acquired | : 23/04/2015 12:25:54 |
| Data Processed | : 23/04/2015 13:05:57 |

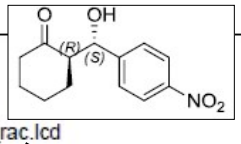


**<Chromatogram>**

C:\LabSolutions\Data\Profa Andrea\Elaine\Aldol_rac.lcd

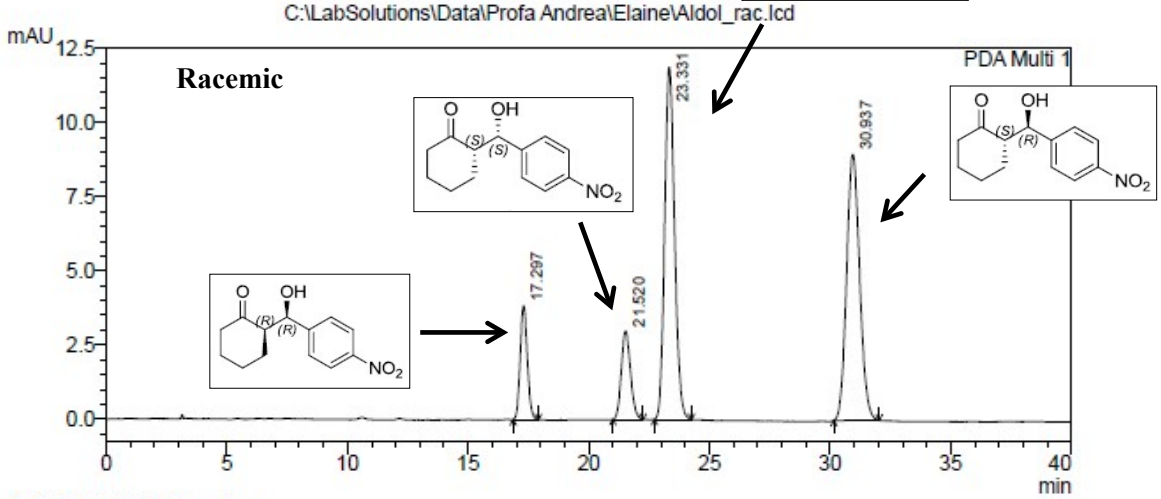


1 PDA Multi 1/254nm 4nm

PeakTable

PDA Ch1 254nm 4nm

| Peak# | Ret. Time | Area | Height | Area % | Height % |
|---|---|---|---|---|---|
| 1 | 17.297 | 79314 | 3838 | 9.523 | 13.878 |
| 2 | 21.520 | 78611 | 2976 | 9.438 | 10.759 |
| 3 | 23.331 | 338095 | 11874 | 40.594 | 42.930 |
| 4 | 30.937 | 336857 | 8970 | 40.445 | 32.433 |
| Total | | 832876 | 27658 | 100.000 | 100.000 |

# ==== Shimadzu LCsolution Analysis Report ====

C:\LabSolutions\Data\Profa Andrea\Bruna\84(0,5).lcd

| | |
|---|---|
| Acquired by | : Admin |
| Sample Name | : 84(0,5) |
| Sample ID | : 84(0,5) |
| Tray# | : 1 |
| Vail # | : 2 |
| Injection Volume | : 1 uL |
| Data File Name | : 84(0,5).lcd |
| Method File Name | : Chiral_AD-H_10-90_1.0mL-min-40min-08out2014.lcm |
| Batch File Name | : batch-08out2014.lcb |
| Report File Name | : Default.lcr |
| Data Acquired | : 23/04/2015 13:06:21 |
| Data Processed | : 23/04/2015 13:46:26 |

**<Chromatogram>**

C:\LabSolutions\Data\Profa Andrea\Bruna\84(0,5).lcd

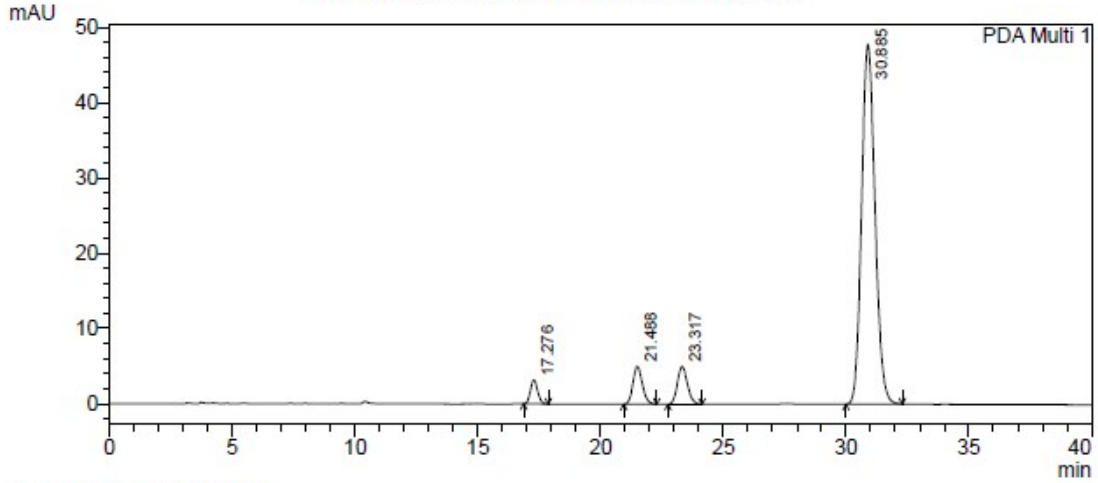


1 PDA Multi 1/254nm 4nm

PeakTable

PDA Ch1 254nm 4nm

| Peak# | Ret. Time | Area | Height | Area % | Height % |
|---|---|---|---|---|---|
| 1 | 17.276 | 65605 | 3188 | 3.045 | 5.226 |
| 2 | 21.488 | 133506 | 4995 | 6.196 | 8.190 |
| 3 | 23.317 | 142057 | 5000 | 6.593 | 8.197 |
| 4 | 30.885 | 1813616 | 47814 | 84.167 | 78.387 |
| Total | | 2154784 | 60996 | 100.000 | 100.000 |

## REFERENCES


1. J. S. Pedersen, *Adv. Colloid Interface Sci.*, 1997, **70**, 171-210.
2. T. Zemb and P. Lindner, *Neutrons, X-rays and Light: Scattering Methods Applied to Soft Condensed Matter*, Elsevier, Amsterdam, 2002.
3. G. Beaucage, *J. Appl. Crystallogr.*, 1996, **29**, 134-146.
4. J. Teixeira, *J. Appl. Crystallogr.*, 1988, **21**, 781-785.
5. I. Bressler, J. Kohlbrecher and A. F. Thünemann, *J. Appl. Crystallogr.*, 2015, **48**, 1587-1598.
6. C. M. Sorensen and G. M. Wang, *Phys. Rev. E*, 1999, **60**, 7143-7148.
7. M. Abramowitz and I. A. Stegun, *Handbook of mathematical functions, with formulas, graphs, and mathematical tables*, Dover Publications, New York, 1965.
8. E. Butkov, *Mathematical Physics*, Addison-Wesley Publishing Company, Reading-Massachusetts, 1968.
9. D. J. Kinning and E. L. Thomas, *Macromolecules*, 1984, **17**, 1712-1718.
10. J. K. Percus and G. J. Yevick, *Phys. Rev.*, 1958, **110**, 1-13.
11. N. Mase, Y. Nakai, N. Ohara, H. Yoda, K. Takabe, F. Tanaka and C. F. Barbas, III, *J. Am. Chem. Soc.*, 2006, **128**, 734-735.